Gravity Waves Associated with Jet/Front Systems:

Characteristics of Gravity Waves Revealed in a Baroclinic Instability Simulation

Hye-Yeong Chun[1] and Young-Ha Kim[2]

[1]*Yonsei University, Korea*

[2]*Ewha Womans University, Korea*

2016 SPARC Gravity Wave Symposium / May 16, 2016

Introduction

- Gravity waves (GWs) at high latitudes have a significant impact on the shape and magnitude of the polar jet in the middle atmosphere.
- Mountains are one of the main sources of high-latitude GWs. However, momentum deposited by mountain GWs does not fully account for the momentum required to form the polar jet structure as observed (*Sato et al.* 2012; *Choi and Chun* 2013).
- Jet-front systems are considered as a feasible source of high-latitude GWs, based on observational and modeling studies (e.g., *Uccellini and Koch* 1987; *O'Sullivan and Dunkerton* 1995; *Plougonven and Zhang* 2014).
- Characteristics of the jet-front GWs observed (e.g., *Guest et al.* 2000; *Plougonven et al.* 2003) : $\lambda_h \sim$ **50–500 km** / $\lambda_z \sim$ **1–7 km** / $\omega_i \sim$ **1–3***f*

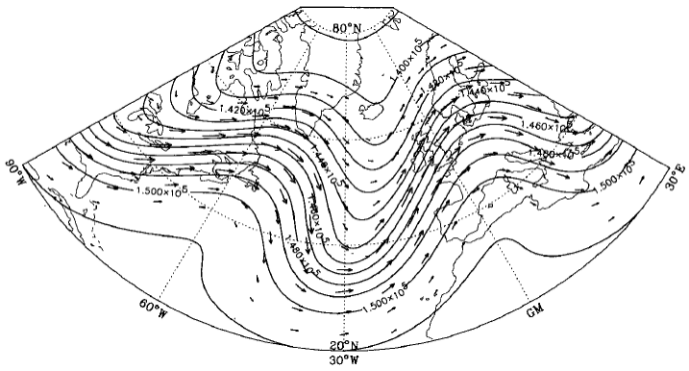

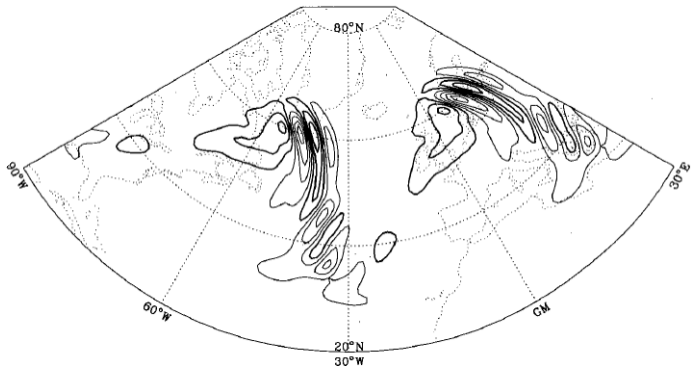

GWs at 130 hPa simulated by *O'Sullivan and Dunkerton* (1995): Φ and divergence fields

Introduction

- As the jet-front systems are likely to associate with baroclinic waves and their instability, modeling studies have often involved simulating baroclinic life cycles (e.g., *Zhang* 2004; *Plougonven and Snyder* 2007, PS07).
  - ✓ (peak) values of the GW characteristics : in a similar range with that from the observations
  - ✓ PS07 showed that the phase speed of the GW is the same as that of the baroclinic waves in their cases.
  - ✓ Many studies have focused on cases in which baroclinic waves grow fast in the upper troposphere.
- From the perspective of parameterizing GWs, it is important to know the **spectral shapes** of the waves, particularly the horizontal phase-velocity spectrum (or vertical-wavenumber spectrum).
- Provided that the GWs excited near the surface can have a large vertical wavelength (PS07) and thus have potential to propagate far vertically, **low-level baroclinic instability cases** are also of interest.

In this study, we investigate the spectral characteristics of GWs simulated in an idealized low-level baroclinic instability case.

In addition, for this case we qualitatively examine large-scale indicators of GW generation which have been used or derived for parameterization purposes.

Introduction

- **Experiment description**
- **Results**
  - **Baroclinic wave evolution**
  - **GW detection**
  - **Characteristics of GWs**
  - **Vertical propagation aspects of GWs**
  - **Discussion on GW generation /**
    Examination of large-scale indicators of the GW generation
- **Summary and discussion**

Experiment

Experiment case	*Jablonowski and Williamson* (2006)'s idealized baroclinic instability test case (dry, no topography)
Model	**Global** version of Advanced Research WRF
Resolution	**0.09° x 0.09°** (~10.3 km at Eq.) Δz ~ **200–600 m** at z = 1–12 km (top: 31 km)
Timestep	30 s
Sponge layer	Uppermost 5 km (z > 26 km)
Initial perturbation	Wavenumber-**9** sinusoidal perturbation with a small amplitude at ~50°N near the surface (λ ~ 3000 km)
Time length	7 days
Data analyzed	5-minute u, v, w, T, p, Z at Day 4–7

(*Park et al.*, 2013, MWR)

Zonally symmetric, balanced initial state of JW06

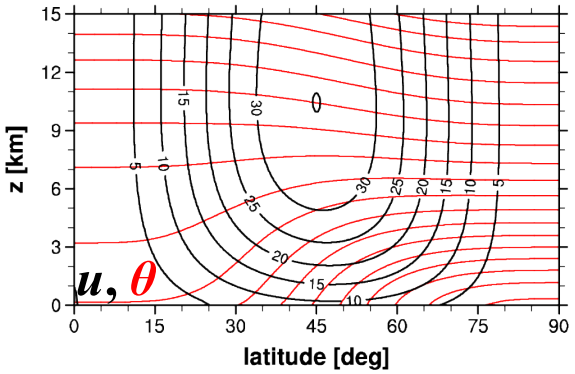

- ✓ peak magnitude of 35 m/s at ~11 km at 45°N
- ✓ maximum $|\nabla T|$ at the surface
- ✓ small vertical shear above the jet core

Definitions

- **Background-flow field** :
  defined at each grid point and time as a spatial running average over the area bounded by the distance (r_a) of 300 km from the grid point

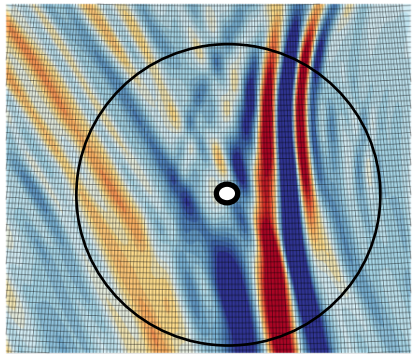

- **Perturbations** :
  defined as a departure from the background field

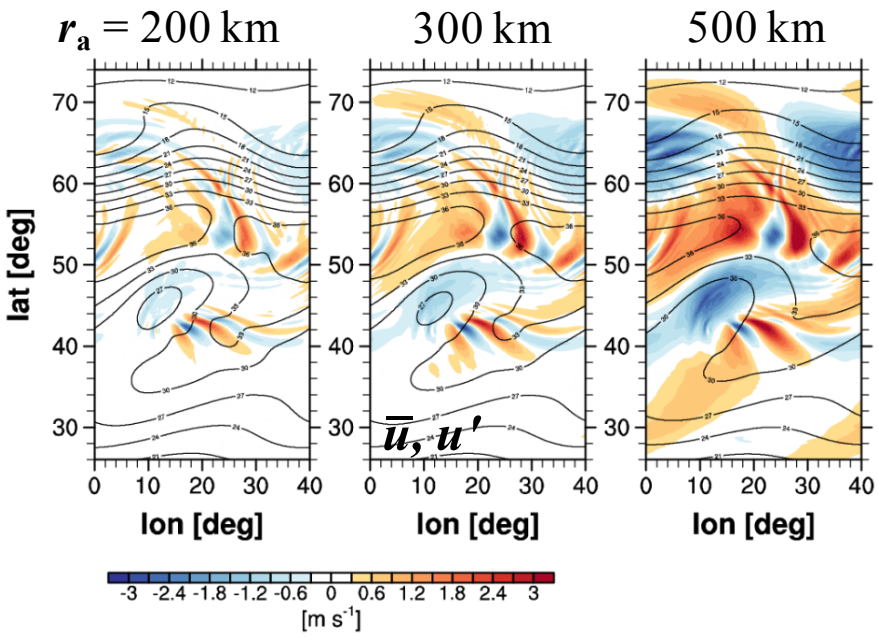

Examples: background (contour) and perturbations (shading) at z = 8 km

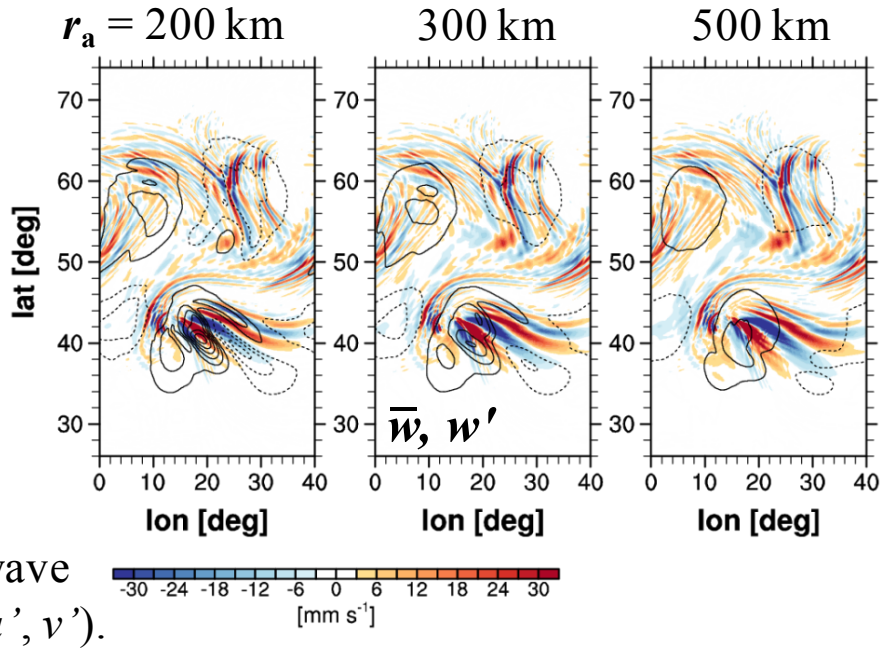

✓ 200 km : too noisy background field

✓ 500 km : A substantial portion of the synoptic wave is included in the perturbation fields (u', v').

Baroclinic wave evolution

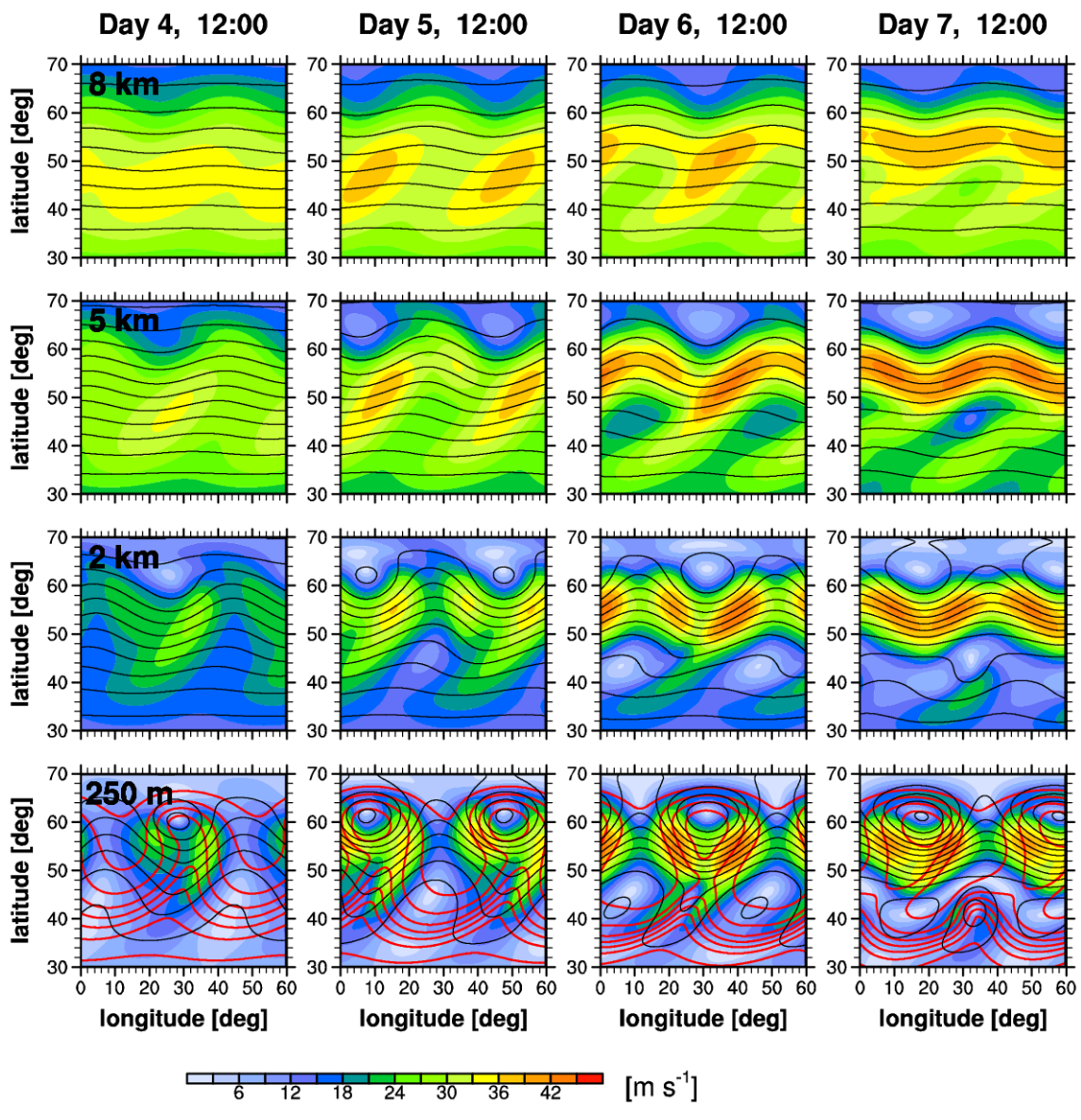

(symmetric for every 40° in longitude)

Background fields :
(shading) $|u_h|$
(black) p
(red) **250-m** θ

- ✓ Day 4 : The amplitude is maximal in 45–60°N at 250 m and decreases with height.
  A low-level jet develops around the trough.
- ✓ Day 5–6 (mature stage) : The warm core at ~60°N begins to be isolated from the midlatitude front by the low-level jet.
- ✓ Day 6–7 (breaking stage) : The surface trough at ~42°N grows away from the higher-latitude trough.
  On Day 7, this isolated secondary low is almost fixed at ~32°E.

Gravity waves revealed at 8 km

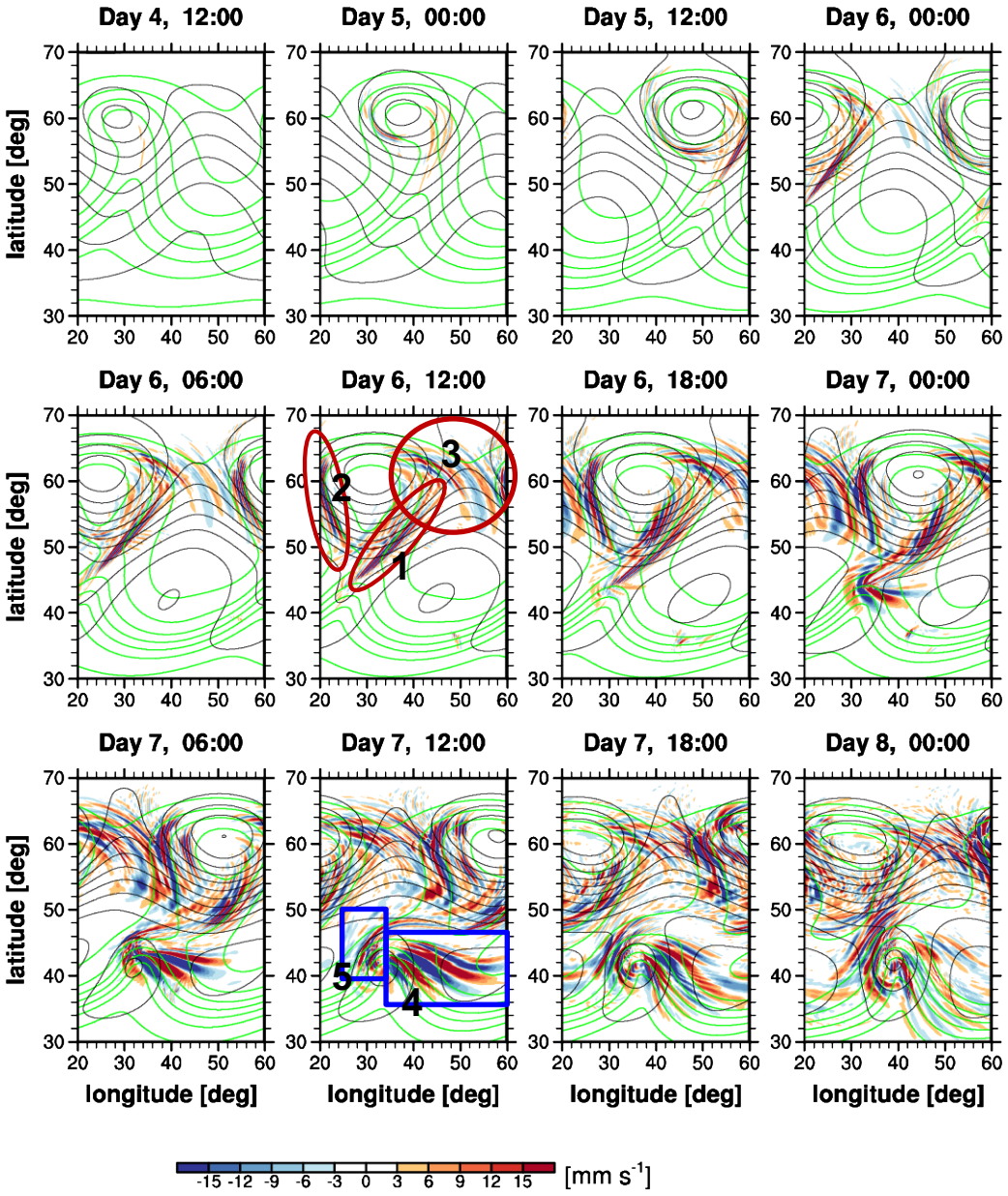

Background *p* at 250 m
***w'* at 8 km**

- ✓ Day 6 : Three major groups of GWs are found with large amplitudes (**W1–W3**).
- ✓ The locations of W1–W3 relative to the phase of the low-level baroclinic wave are maintained throughout the simulation.
- ✓ Day 7 : Another wave groups are detected where the secondary surface low is isolated (**W4** and **W5**).
- ✓ The phase lines of the GWs (except W3) tend to be parallel to the 250-m isentropic lines (green contour).

Gravity waves revealed at 8 km

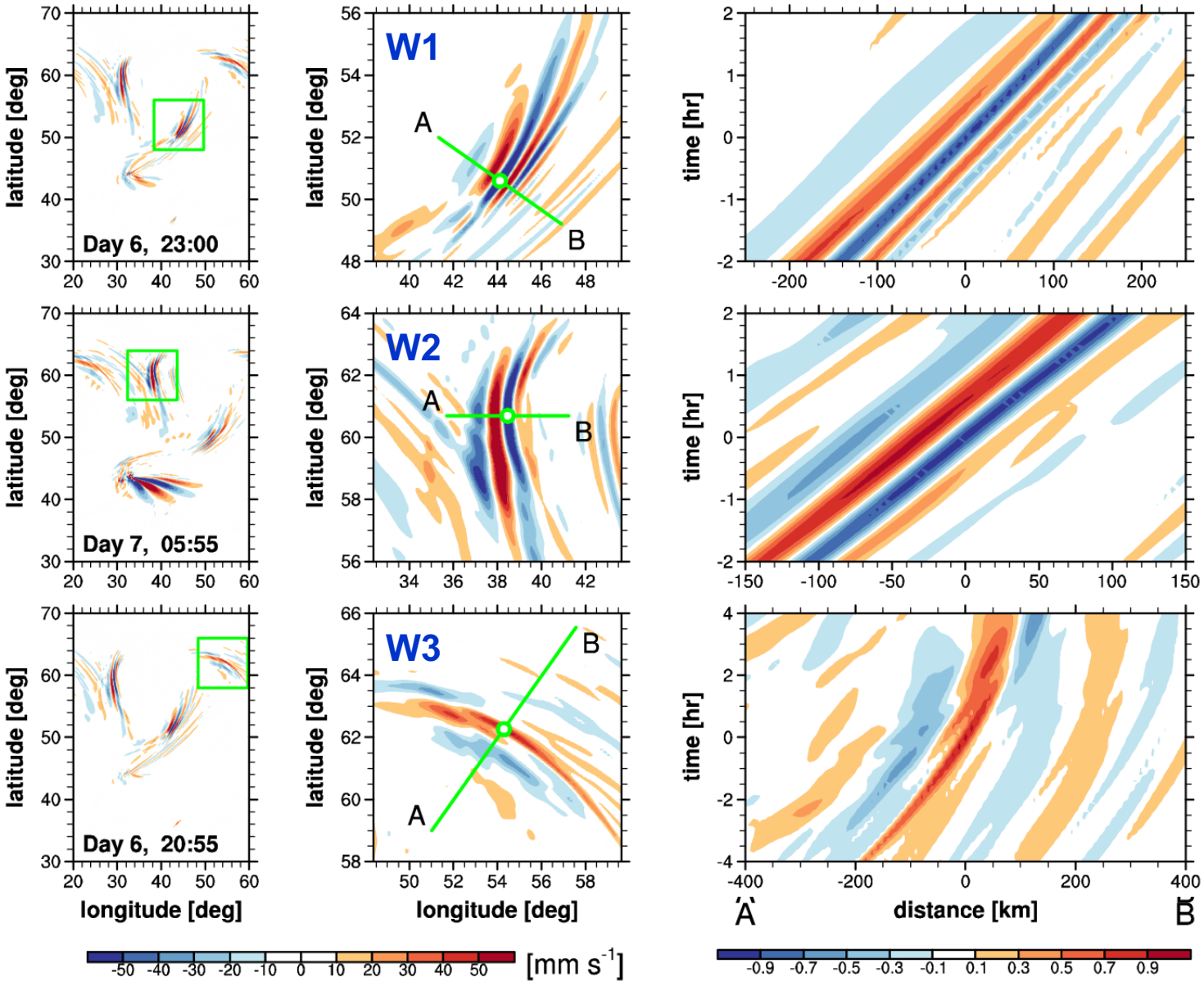

Horizontal close-up view of w' at 8 km (center) and its time cross section (right)

70 km, 19 m/s : λ_h , c_p
60 min : τ

60 km, 15 m/s,
70 min

200 km, 10 m/s
330 min

Gravity waves revealed at 8 km

Horizontal close-up view of *w'* at 8 km (center) and its time cross section (right)

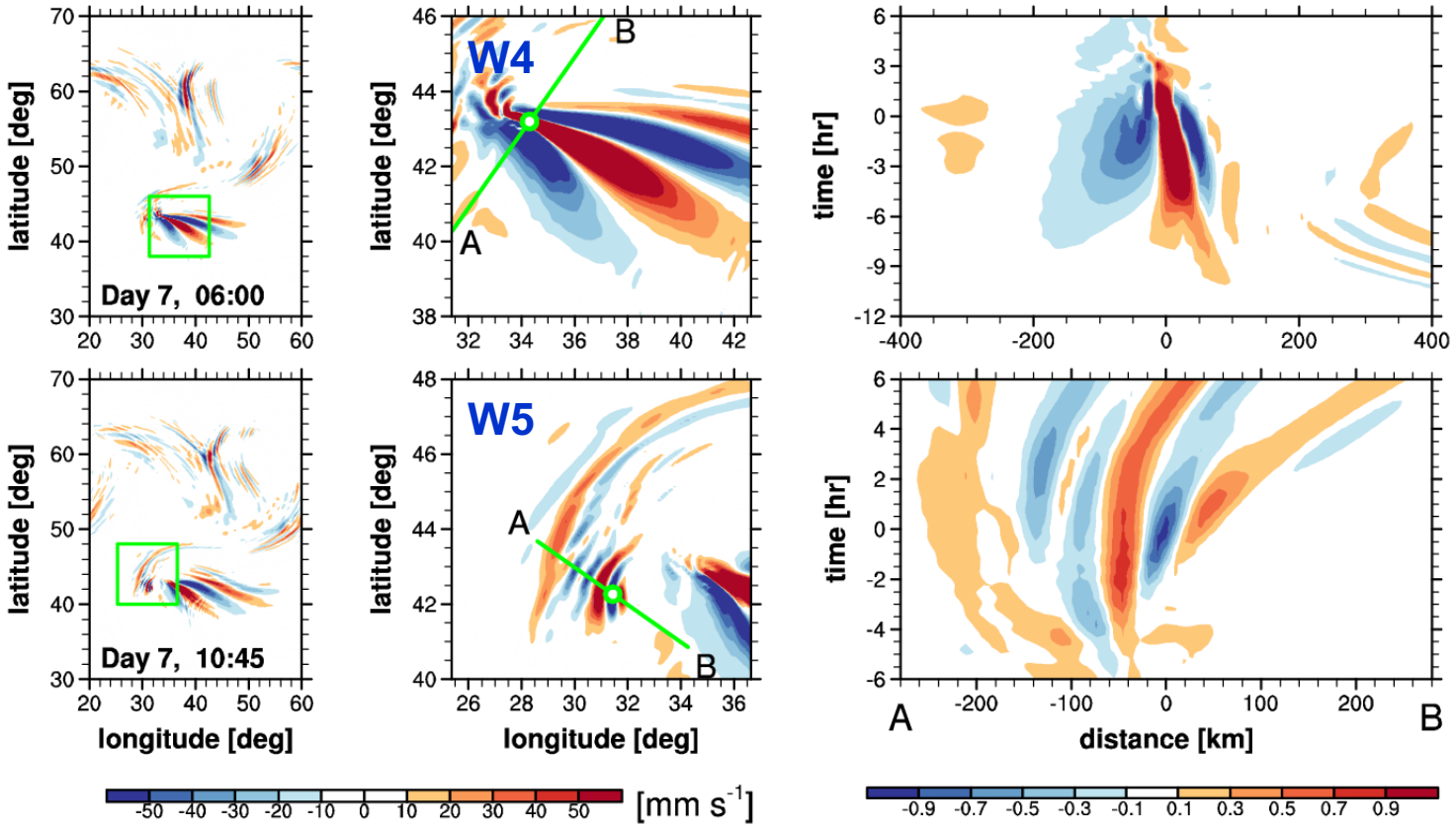

✓ The horizontal wavelength of W4 and phase speeds of W3 and W5 vary significantly with location and time, implying broad spectra of the waves.

Spectral decomposition

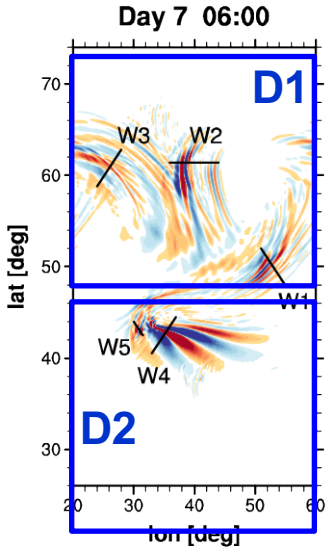

PSD(k, l) of w' at 8 km (12-hr average)

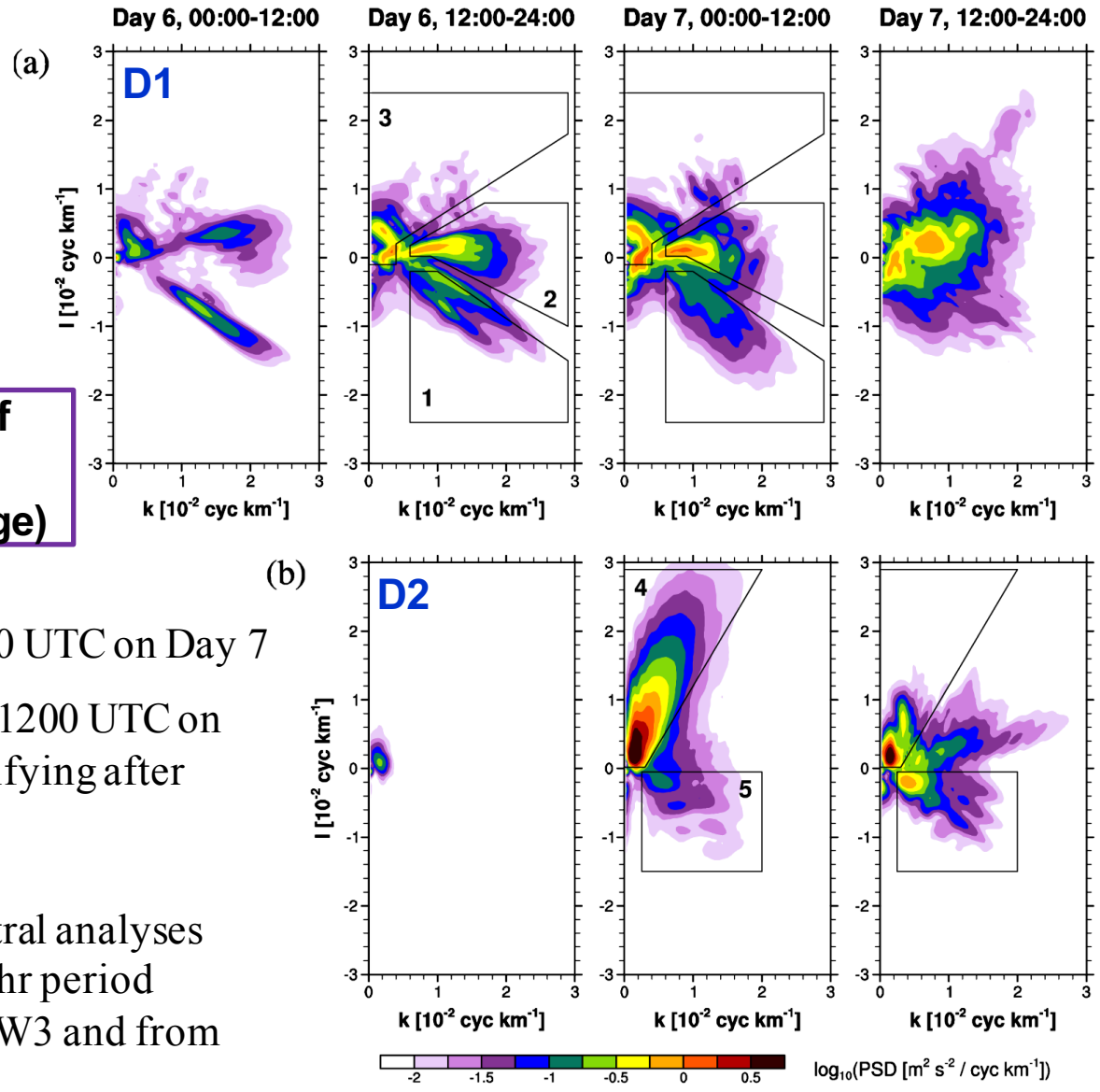

- ✓ D1 : three distinct peaks until 1200 UTC on Day 7
- ✓ D2 : a predominant peak at 0000–1200 UTC on Day 7 ; the second peak amplifying after 1200 UTC on Day 7
- ✓ The wave decomposition and spectral analyses hereafter are performed for the 24-hr period from 1200 UTC on Day 6 for W1–W3 and from 0000 UTC on Day 7 for W4–W5.

Spectral decomposition

Reconstructed *w'* field

To confirm that W1–W5 revealed in the *w'* fields are well represented by the decomposed waves.

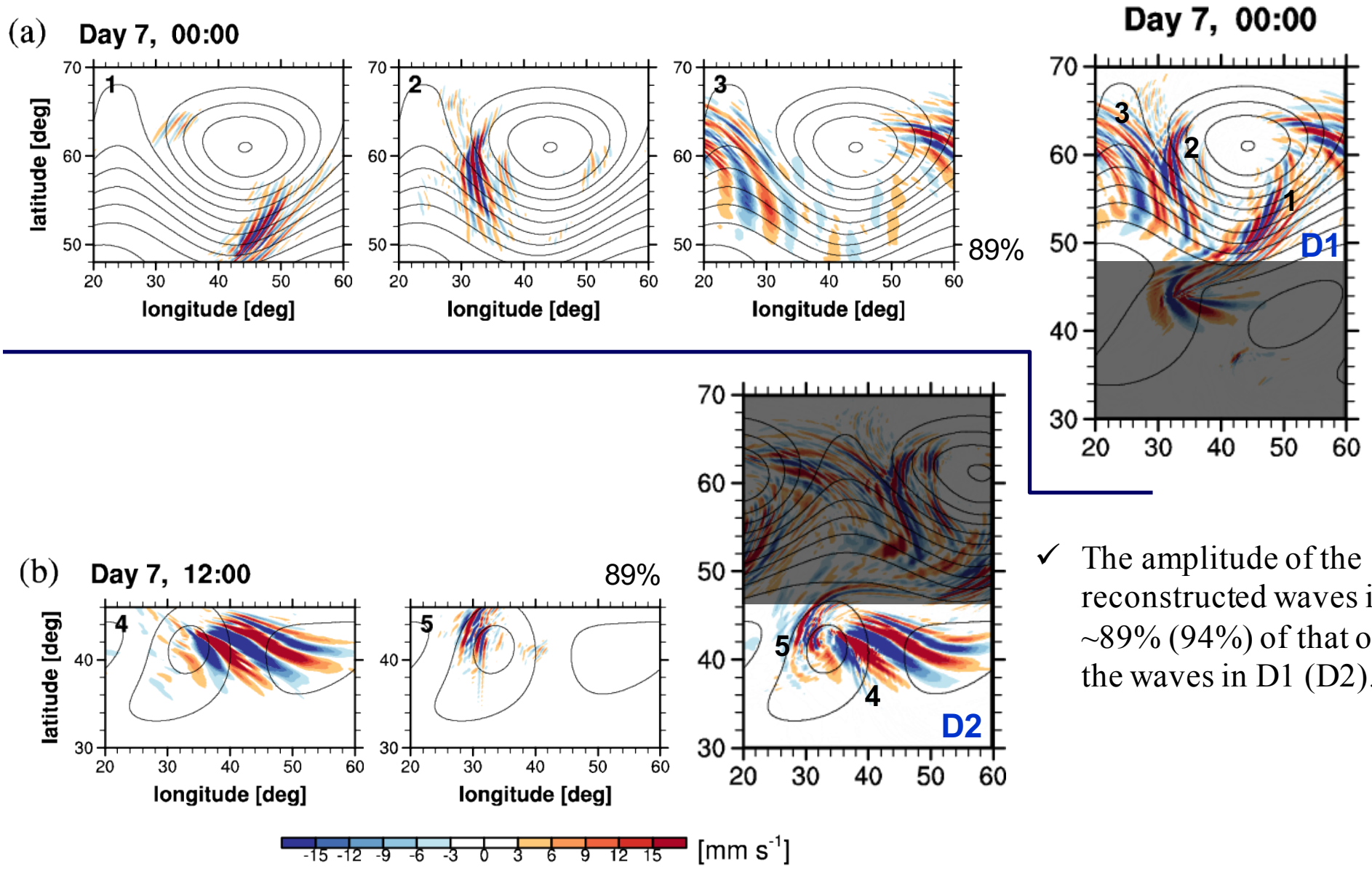

✓ The amplitude of the reconstructed waves is ~89% (94%) of that of the waves in D1 (D2).

GW Characteristics

Wavelength and frequency spectra of *w'* at 8 km for W1–W5

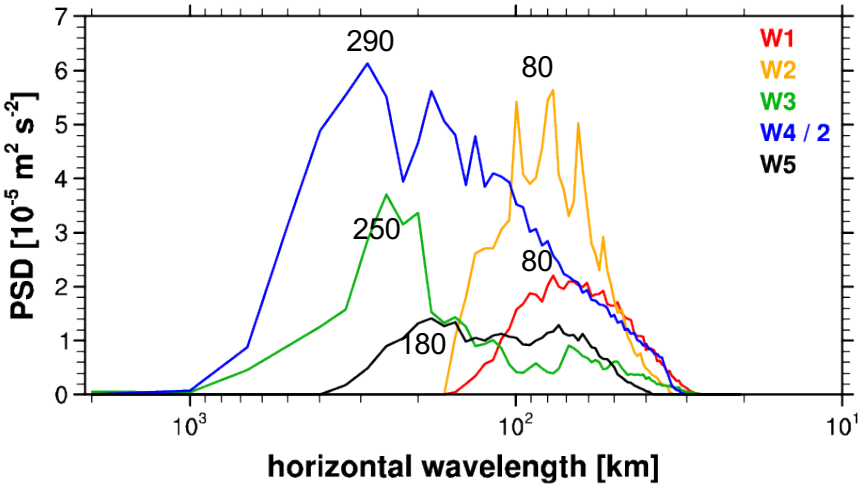

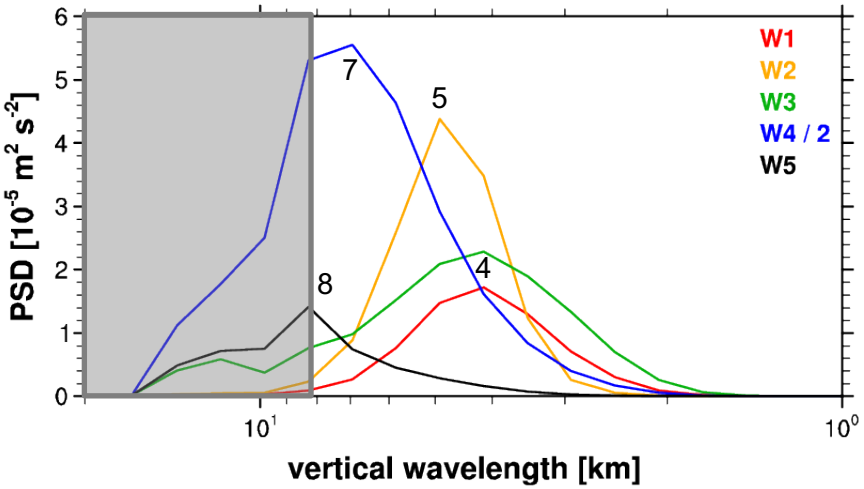

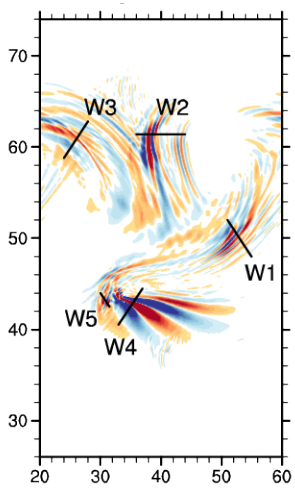

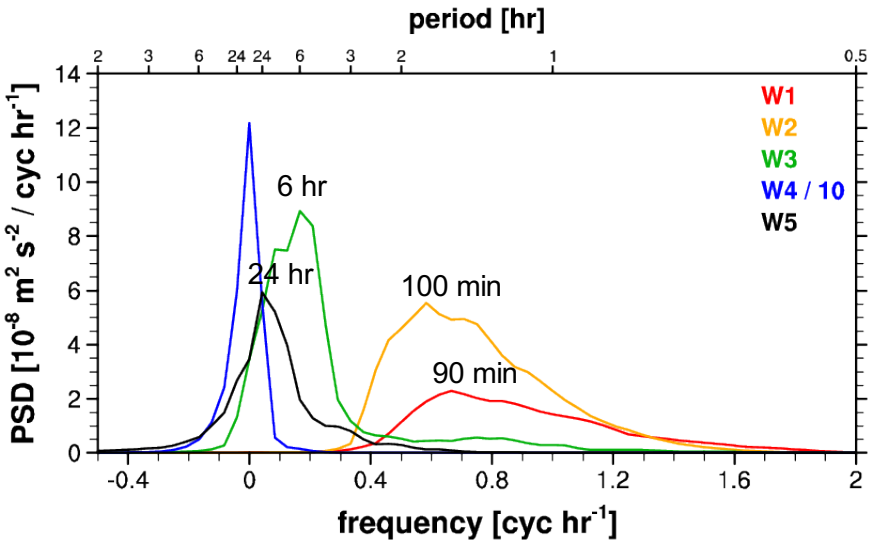

- ✓ The horizontal wavelengths are in the range obtained from the previous studies.
- ✓ The vertical wavelengths generally tend to be greater than those in the previous modeling studies.
  - difference in baroclinic wave structure
  - differing analysis method

GW Characteristics

2-D phase-velocity spectra of w' at 8 km for W1–W5

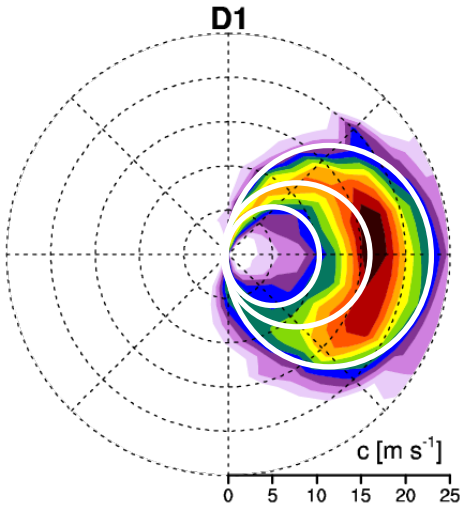

- ✓ The total spectrum in D1 has a continuous, single structure: arc shape.
- ✓ Three possible mechanisms by which the total spectrum in D1 can be made into the arc shape can be suggested.

1) Generation of the waves whose phases are locked to the wave source moving eastward at a speed of ~17 m/s

2) Resonant generation of waves to a certain vertical scale that the wave source would have

3) Considerable amount of critical-level filtering by the background flow

1) isoline of zero phase speed relative t frame movir /s
: c t

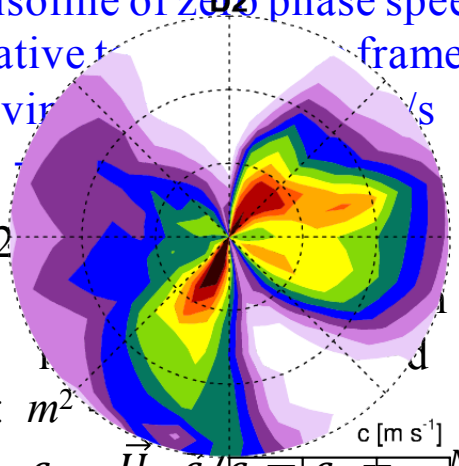

2 1

: m^2 d

$c - \vec{U} \cdot \vec{c}/c = c_i = -N/m$ at source level

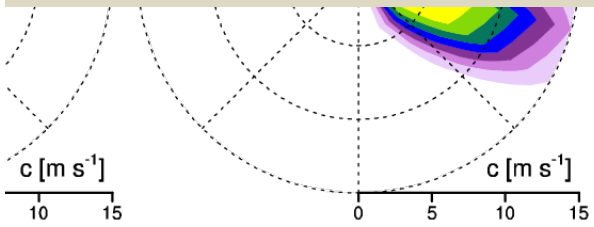

3) critical lines by the westerlies at 24 and 10 m/s
: $c - (24, 0) \cdot \vec{c}/c = c_i = 0$ (and vice versa)

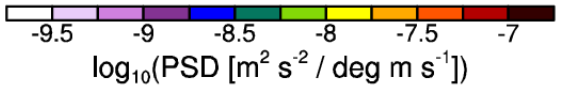

GW Characteristics

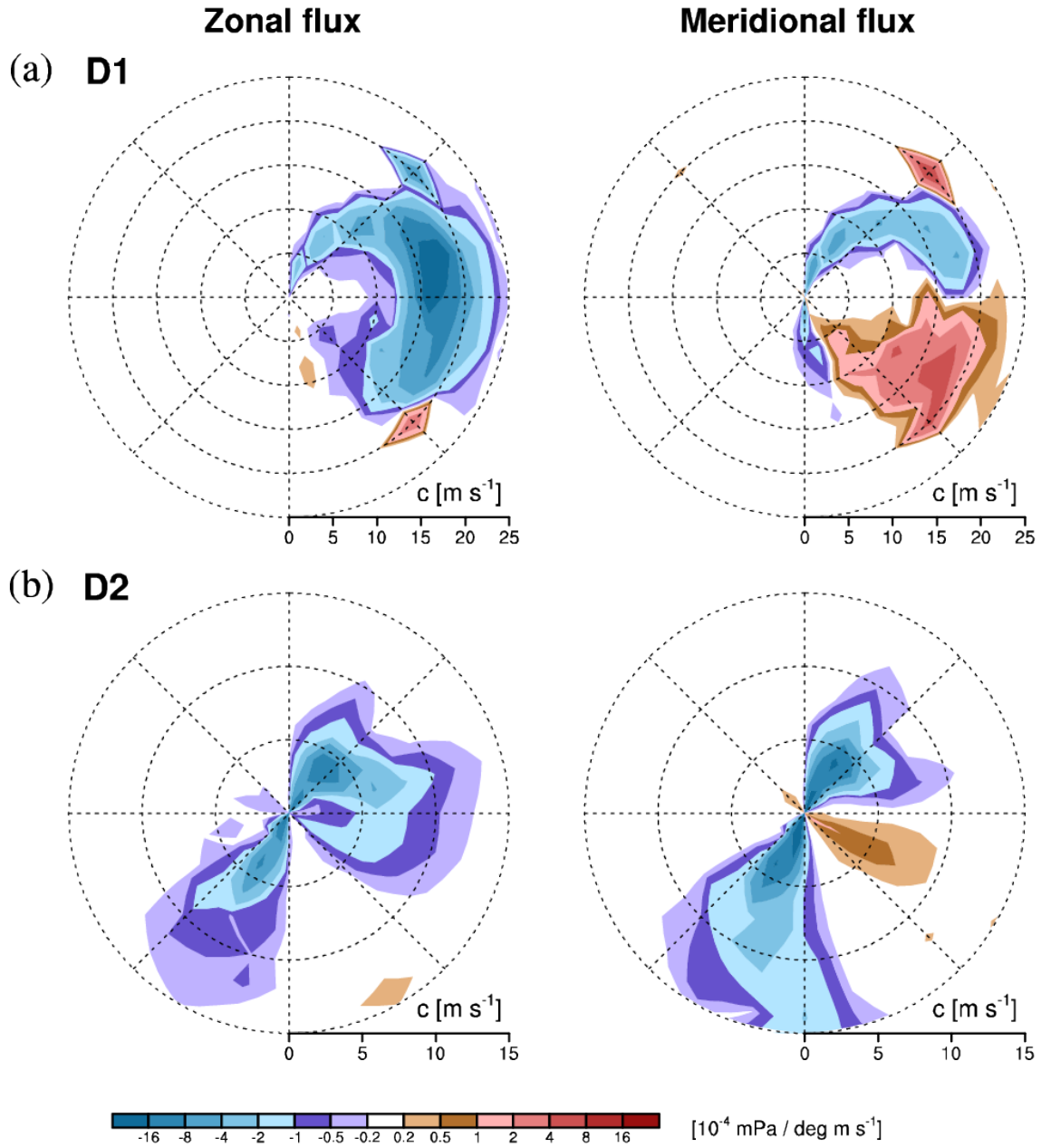

Phase-velocity spectra of GW momentum flux at 8 km for W1–W5

- ✓ The spectral shape of the horizontal momentum flux is similar to that of ***w'***.
- ✓ Negative zonal momentum flux for all W1–W5
- ✓ The signs of the zonal and meridional momentum fluxes all indicate upward propagation of waves (with westward intrinsic phase velocities).

Vertical propagation of GWs

Vertical cross sections of *w'* for W1–W5 (shading) and background wind projected onto the GW phase directions (contour)

Day 7, 00:00

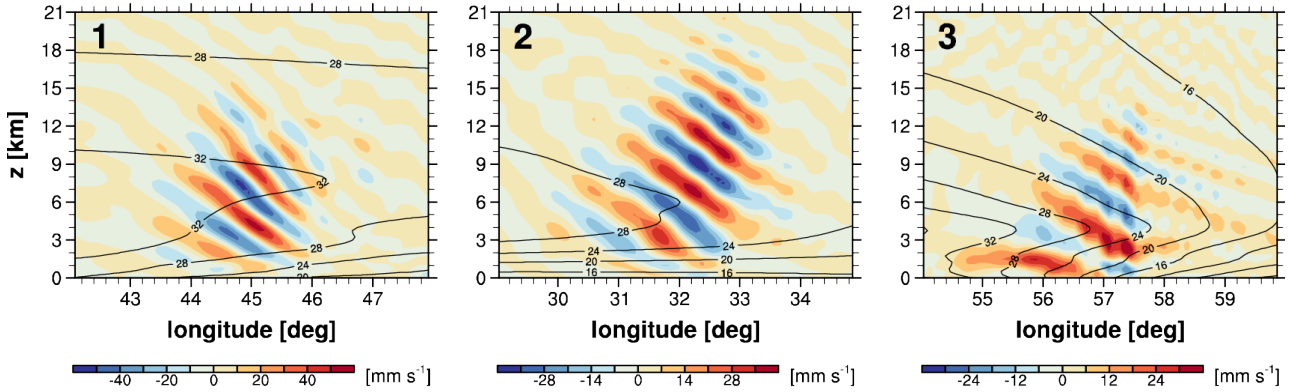

Day 7, 12:00

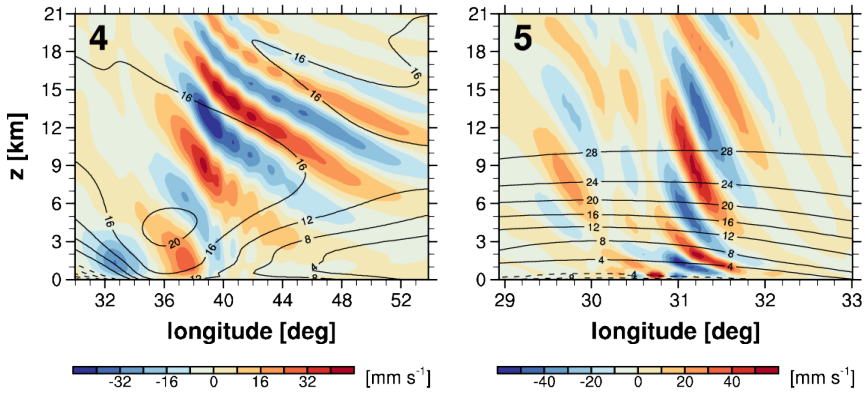

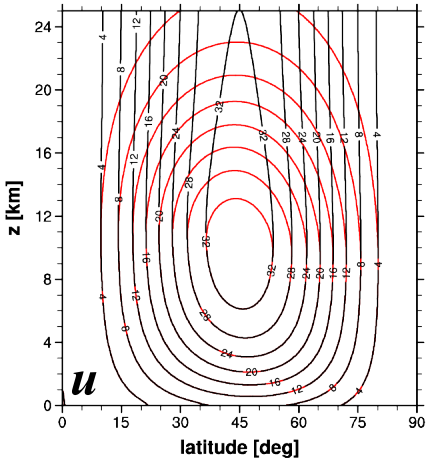

- ✓ The GWs propagate upward and dissipate in the upper troposphere, especially for W1–W3.
- ✓ The critical-level filtering of GWs seems not significant due to the weak shear (**black**). The dissipation might be due to the (implicit) numerical diffusion for the horizontally/vertically small-scale waves (~$7\Delta_z$, $8\Delta_h$).
- ✓ In reality, with more typical background winds (red), W1–W3 must be filtered in their critical layers above the jet core, while the quasi-stationary W4 and W5 could propagate into the stratosphere in wintertime.

Vertical propagation of GWs

PSD(λ_h, z) of w'

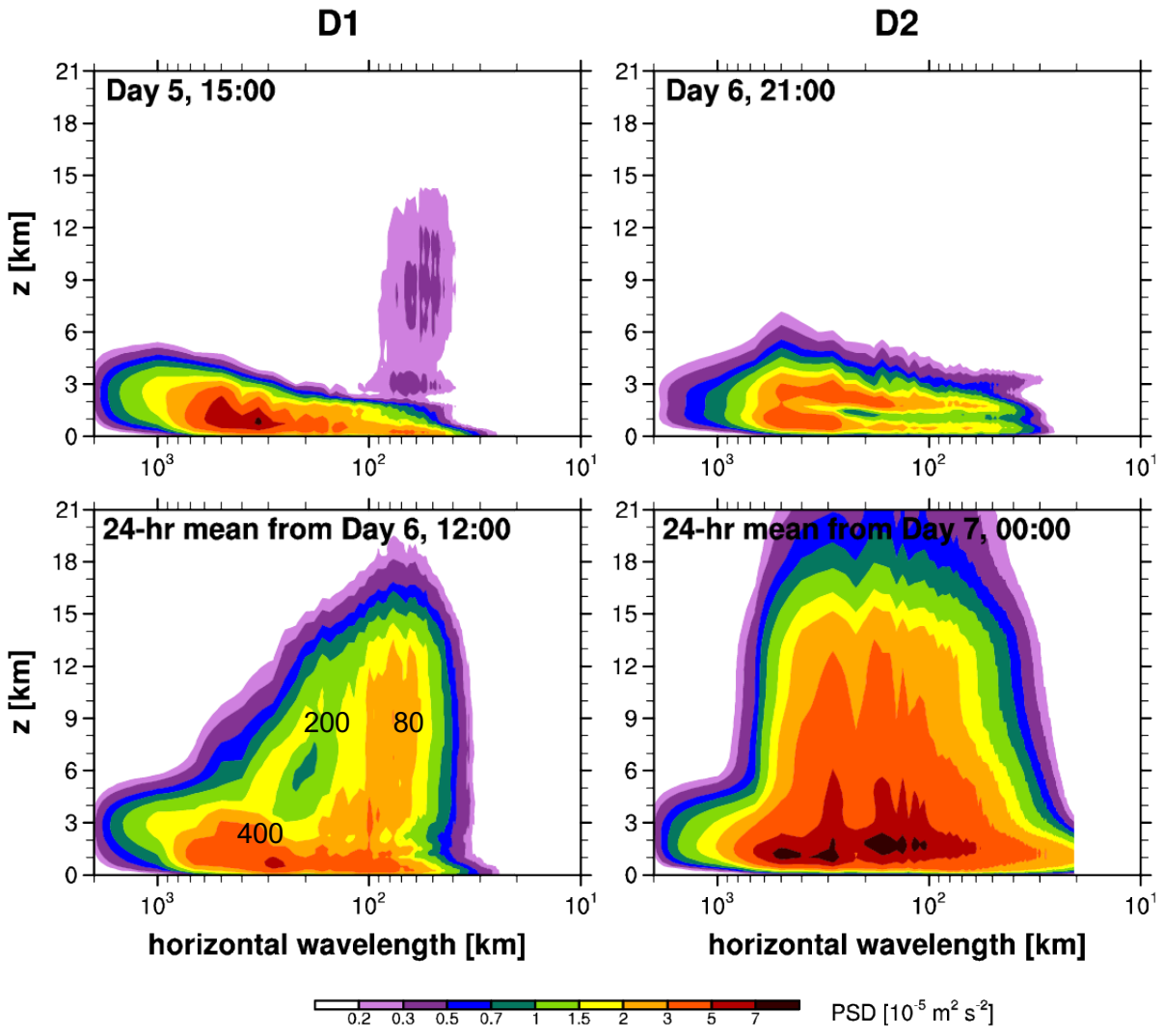

- ✓ In the lower troposphere (1–3 km), energy cascades down from the larger scales.
- ✓ In D1, small-scale waves (< 100 km) propagate fast into the middle troposphere.
- ✓ On Day 6 (when the low-level jet becomes strong), some medium-scale (400 km) waves (W3) propagate upward. The wavelength of W3 is shortened during the propagation.
- ✓ In D2, W4 and W5, with the broad range of wavelength, can propagate upward because of their quasi-stationarity (large intrinsic phase speed).

GW generation in the lower troposphere

w' (shading) and 250-m total θ (contour)

background θ and u_h

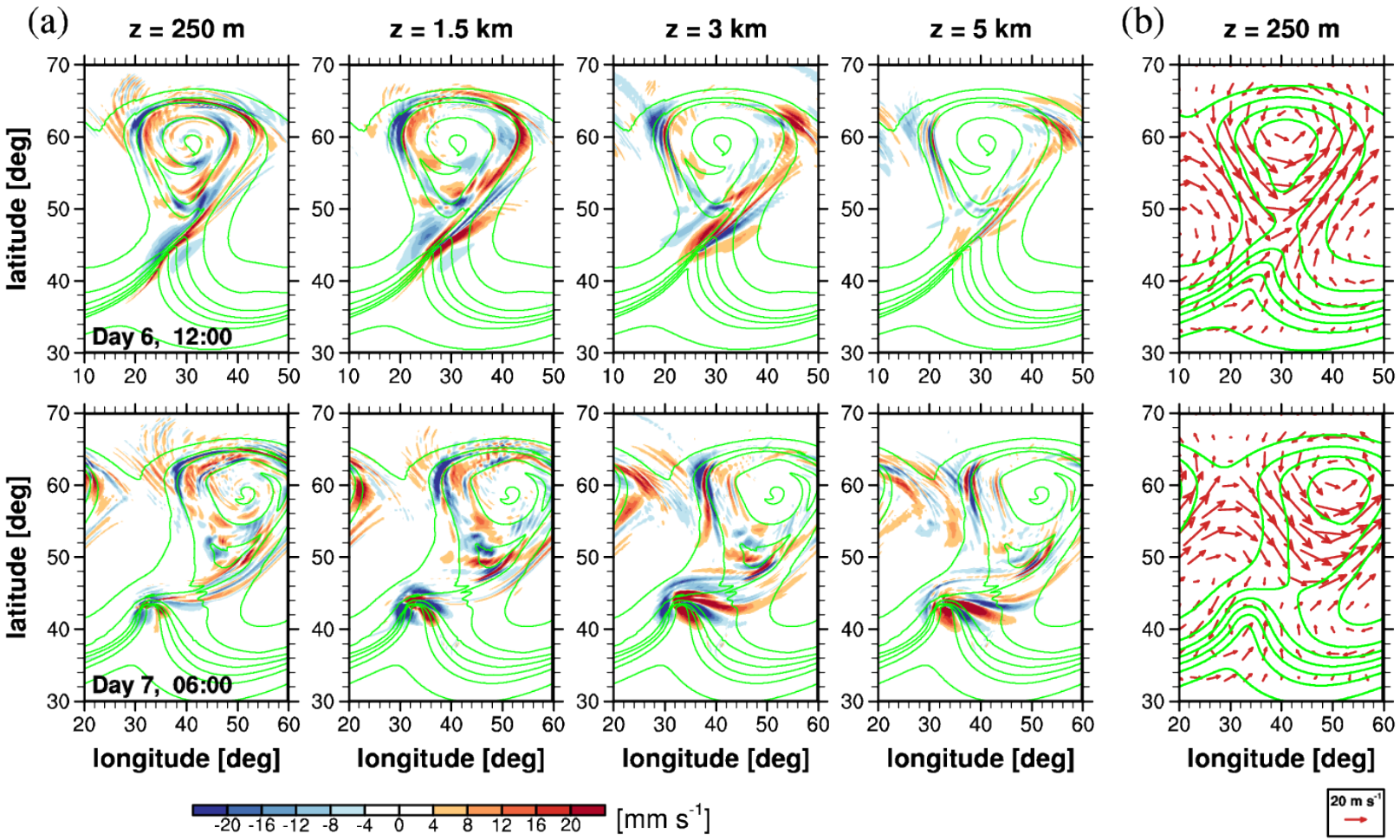

✓ The GWs are emitted from the surface fronts, whose phases are locked to the isentropes following the fronts. This also explains the phase-velocity spectra of the GWs in D1 and D2.

GW generation in the lower troposphere

Frontogenesis function (calculated using the background-flow variables)

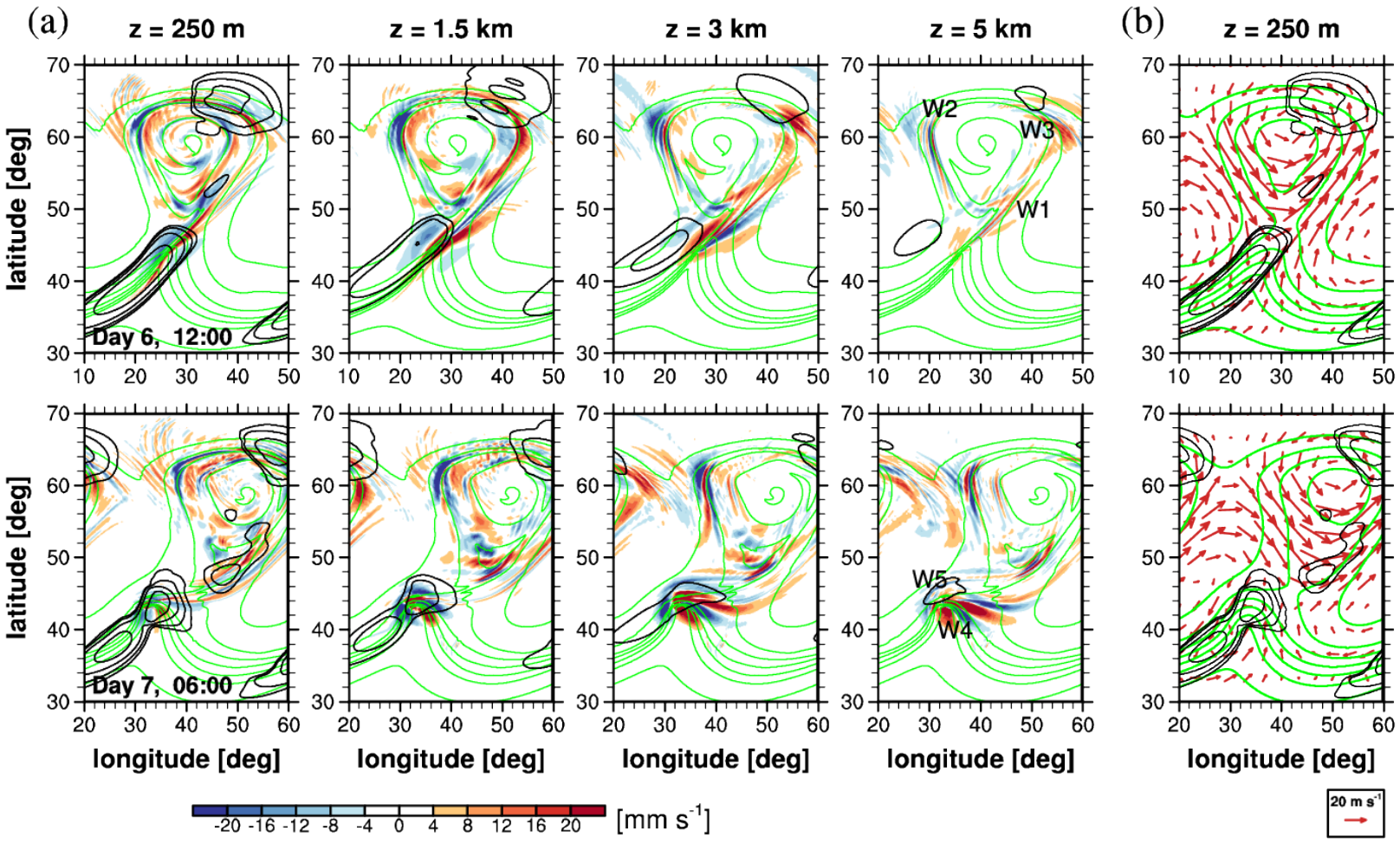

$$\mathrm{FF} \equiv \frac{1}{2}\frac{\mathrm{D}}{\mathrm{D}t}|\nabla\theta|^2 = -\left(\frac{1}{a\cos\phi}\frac{\partial\theta}{\partial\lambda}\right)^2\left(\frac{1}{a\cos\phi}\frac{\partial u}{\partial\lambda} - \frac{v\tan\phi}{a}\right) - \left(\frac{1}{a}\frac{\partial\theta}{\partial\phi}\right)^2\frac{1}{a}\frac{\partial v}{\partial\phi} - \frac{1}{a^2\cos\phi}\frac{\partial\theta}{\partial\lambda}\frac{\partial\theta}{\partial\phi}\left(\frac{1}{a\cos\phi}\frac{\partial v}{\partial\lambda} + \frac{1}{a}\frac{\partial u}{\partial\phi} + \frac{u\tan\phi}{a}\right)$$

GW generation in the lower troposphere

Residual of the nonlinear balance equation

background p

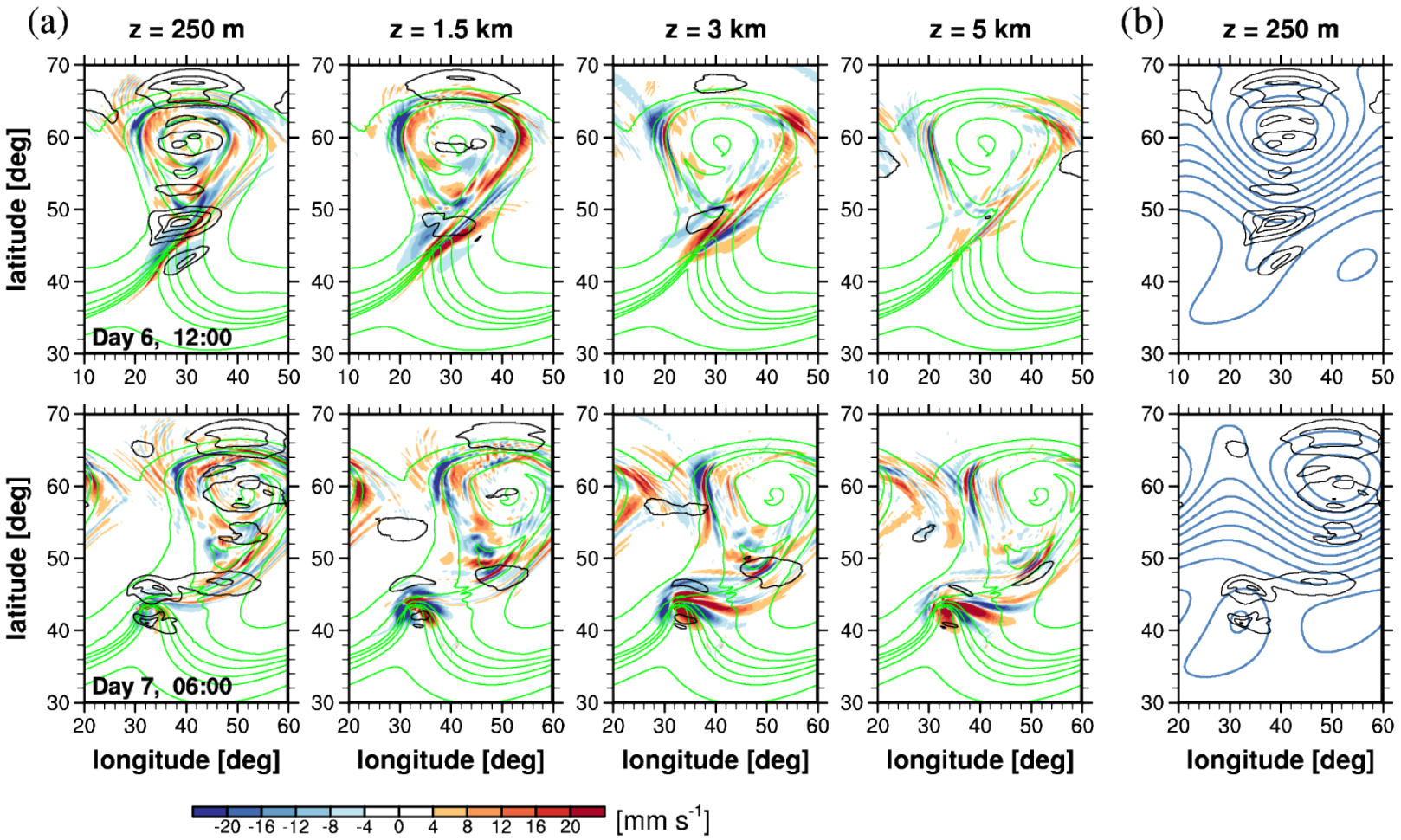

$$\Delta\mathrm{NBE} = f\varsigma - \beta u + \nabla\cdot(\mathrm{PGF}) + 2\mathrm{J}(u,v) + \cdots$$

GW generation in the lower troposphere

Large-scale forcing term of GW derived in Plougonven and Zhang (2007)

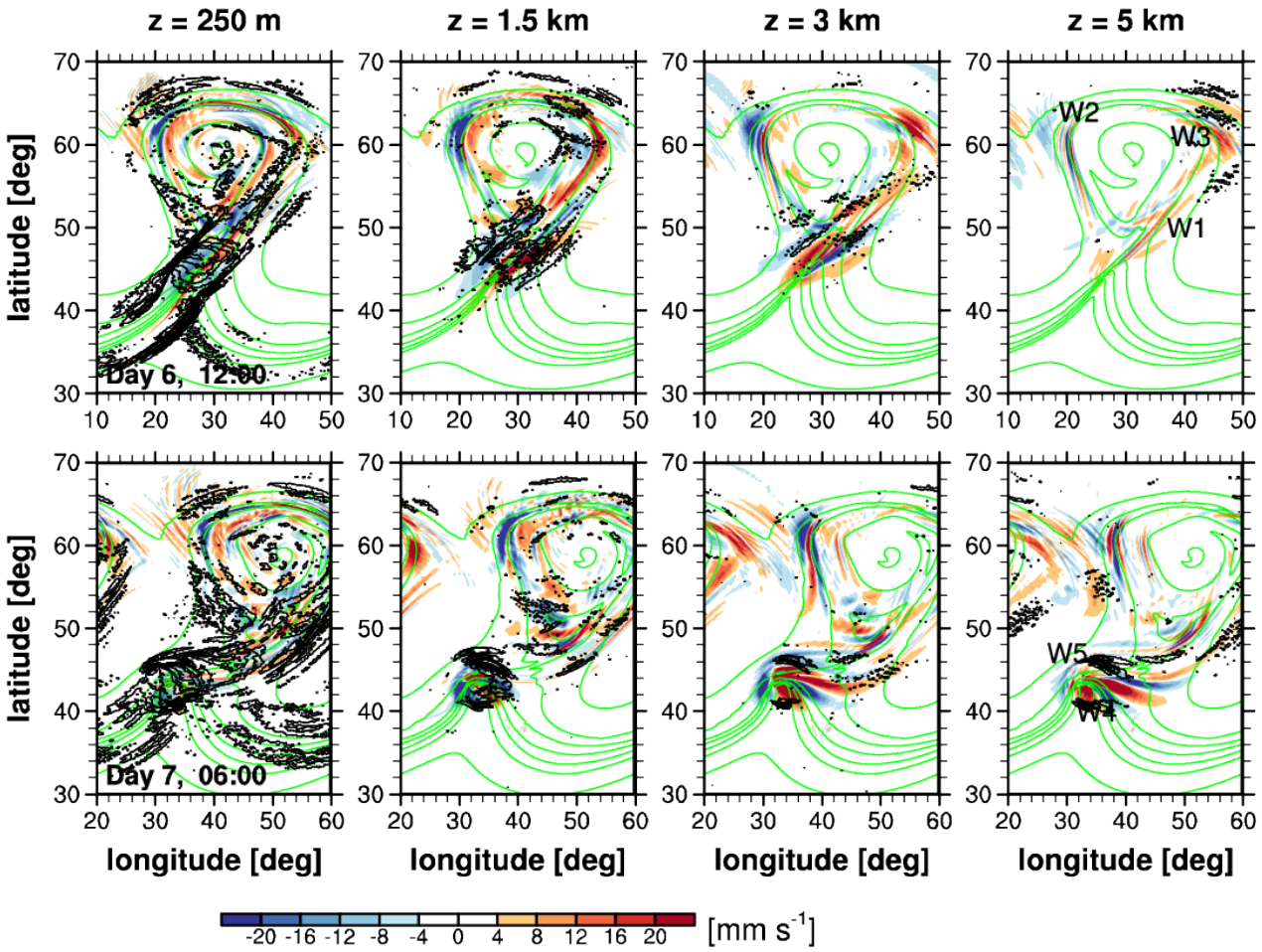

$$[(D_\gamma^2 + f^2)\partial_{zz} + N^2\Delta_H]w^{*\prime} = \boxed{-D_\gamma\partial_z\Delta_{\mathrm{NBE}} + f\partial_z\mathcal{A}_{1,\zeta^*} - \frac{g}{\theta_0}\Delta_H\mathcal{A}_{0,\theta^*},} \quad (15a)$$

$$\Delta_{\mathrm{NBE}} = \overline{\zeta}^* f - \Delta_H\overline{\phi}^* - \beta\overline{u}^* - 2\mathcal{J}(\overline{v}^*, \overline{u}^*), \quad (15b)$$

$$\mathcal{A}_{1,\zeta^*} = (\partial_t + \overline{\mathbf{u}}_H^*\cdot\nabla)\overline{\zeta}^* + f\overline{\delta}^* + \beta\overline{v}^*, \quad \text{and} \quad (15c)$$

$$\mathcal{A}_{0,\theta^*} = (\partial_t + \overline{\mathbf{u}}^*\cdot\nabla)\overline{\theta}^* + \overline{w}^*\partial_z\Theta^*, \quad (15d)$$

✓ More detailed examination on large-scale indicators is required.

Summary and discussion

Characteristics of GWs simulated in an idealized low-level baroclinic instability case are investigated.

	W1	W2	W3	W4	W5
Propagation direction	southeast	east	northeast	quasi-stationary	southeast
Horizontal wavelength [km]	40–110	50–120	70–400	70–400	60–220
	80	**80**	**250**	**290**	**180**
Period	44–110 min	53–130 min	1.6–24 h	$\gtrsim$ 12 h	$>$ 3 h
	90 min	**100 min**	**6 h**	–	**24 h**
Phase speed [m s^{-1}]	14–19	15–18	4–19	0–4	0–9
	17	**17**	**13**	**0**	**2**
Vertical wavelength [km]	2.9–6.9	4.1–6.9	2.9–9.8	4.9–12	5.8–14
	4.1	**4.9**	**4.1**	**6.9**	**8.3**
Absolute momentum flux [mPa]	0.083	0.15	0.66	1.2	0.060

- ✓ Three groups of GWs (W1–W3) appear around the high-latitude surface trough at the mature stage of the baroclinic wave.
- ✓ The phase-velocity spectrum of W1–W3 is arc-shaped with a peak at 17 m/s eastward, which is not prevalent for upward propagation of the waves through the tropospheric jet.
- ✓ At the breaking stage of the baroclinic wave, two groups of quasi-stationary GWs (W4 and W5) appear near the surface low isolated in the midlatitudes, which are able to propagate far vertically.

Summary and discussion

- ✓ The surface fronts near the midlatitude low and around the high-latitude trough are found to be the sources of W1–W5, and the moving speed of the fronts determines the phase-velocity spectrum of the GWs (*Snyder et al.* 1993).
- ✓ The vertical wavelength can be approximated using the hydrostatic dispersion relation with the phase speed.
- ✓ It is not clear how the horizontal wavelengths are determined. However, the wavelength spectrum suggests that near the source region, the energy cascades from larger to smaller scales, having a broad, continuous spectrum. Allowance of the upward wave propagation, among those spectral components, may depend on the background condition and thus location/timing of the waves.
- ✓ A substantial change in the horizontal wavelength during propagation is also reported. Ray-tracing methods may be needed to parameterize such waves.

Further studies needed include

- investigation on how the spectral widths of the characteristics are determined
- development/examination of large-scale indicators of GW generation and their relation with GW amplitudes

Kim, Y.-H., H.-Y. Chun, S.-H. Park, I.-S. Song, and H.-J. Choi, 2016: Characteristics of gravity waves generated in the jet-front system in a baroclinic instability simulation. *Atmos. Chem. Phys.*, **16**, 4799–4815.

Thank you for listening

Additional experiment

Initial wind profiles (black: JW06, red: modified)

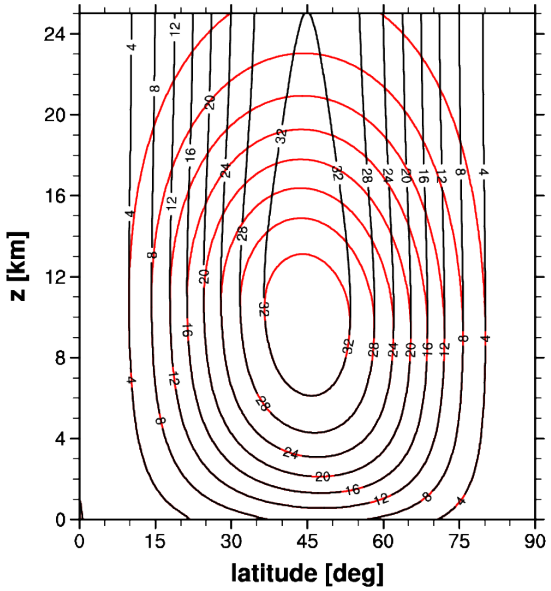

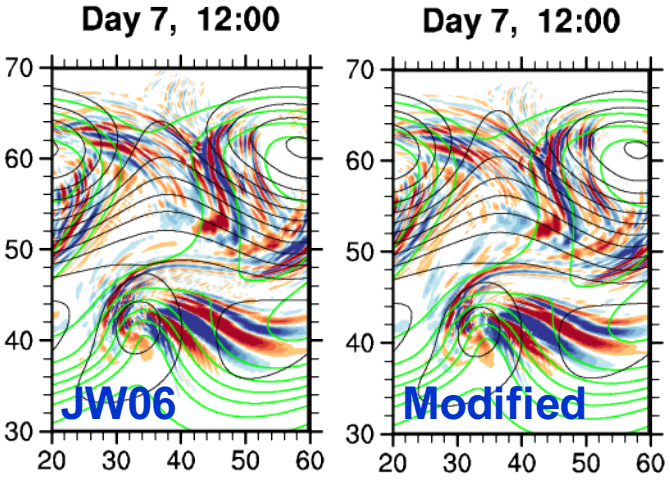

Modified simulation: Vertical cross sections and background wind projected onto the GW phase directions

(a) **Day 7, 00:00**

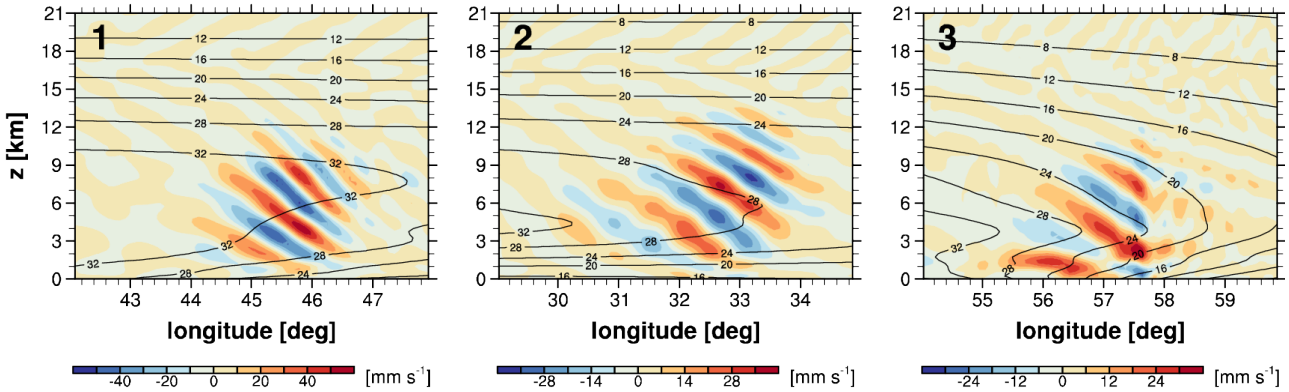

(b) **Day 7, 12:00**

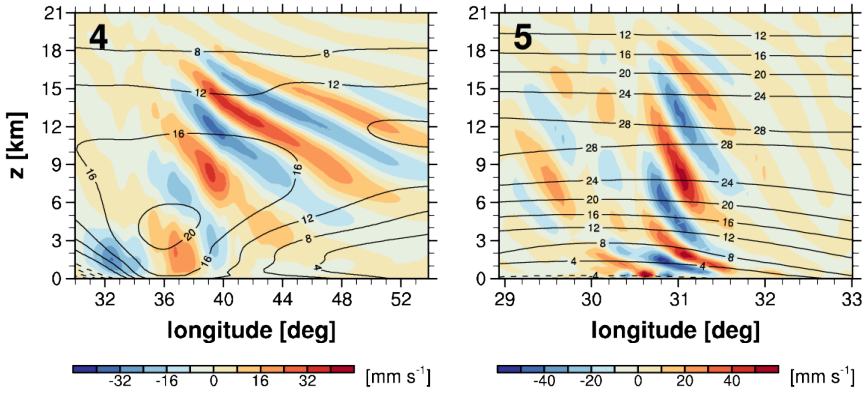

- ✓ Virtually identical results below ~8 km
- ✓ More dissipation in the upper troposphere and stratosphere in the modified simulation than in JW06.

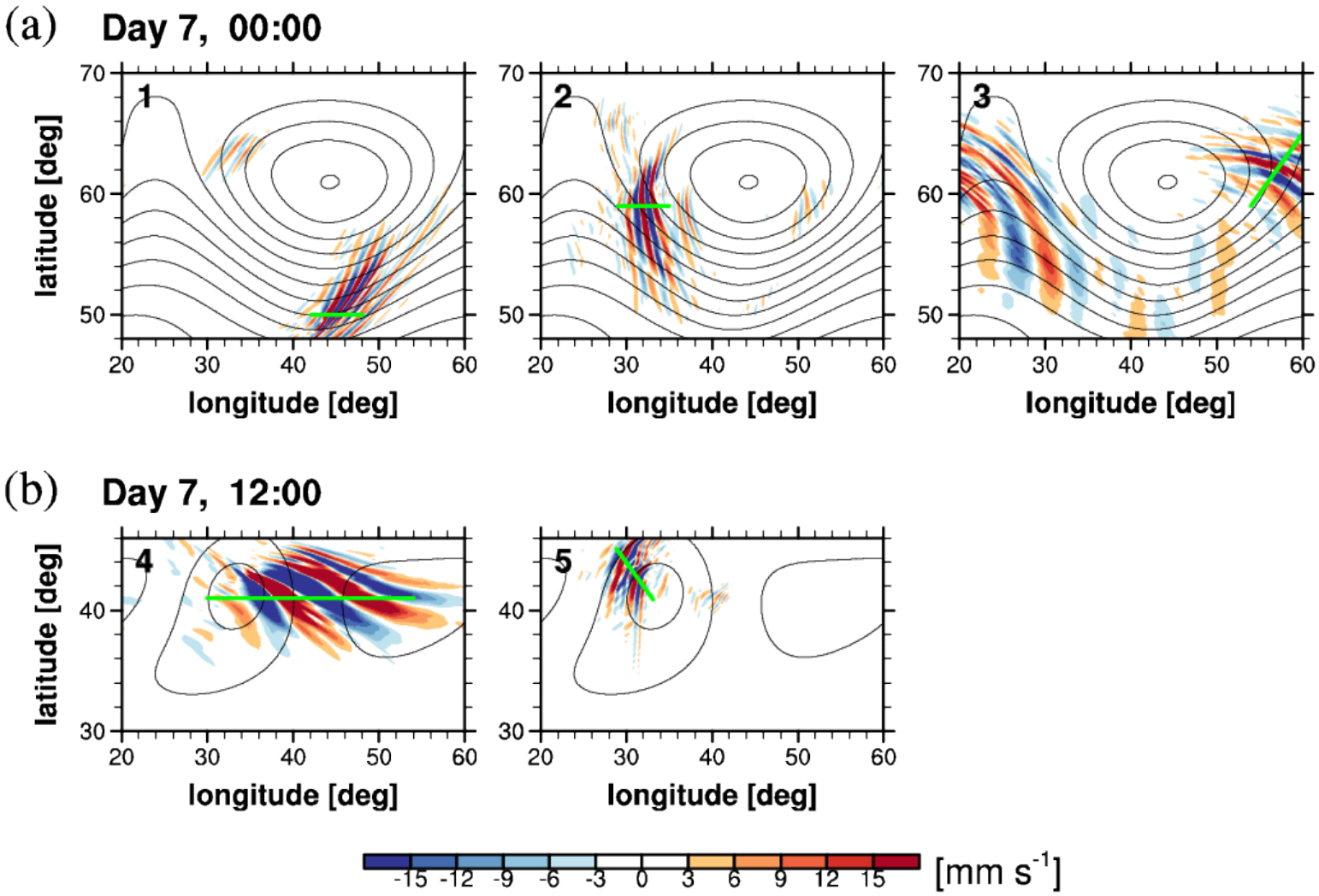
(a) Day 7, 00:00
1
2
3
latitude [deg]
longitude [deg]
70
60
50
20
30
40
50
60
(b) Day 7, 12:00
4
5
40
30
-15 -12 -9 -6 -3 0 3 6 9 12 15
[mm s-1]

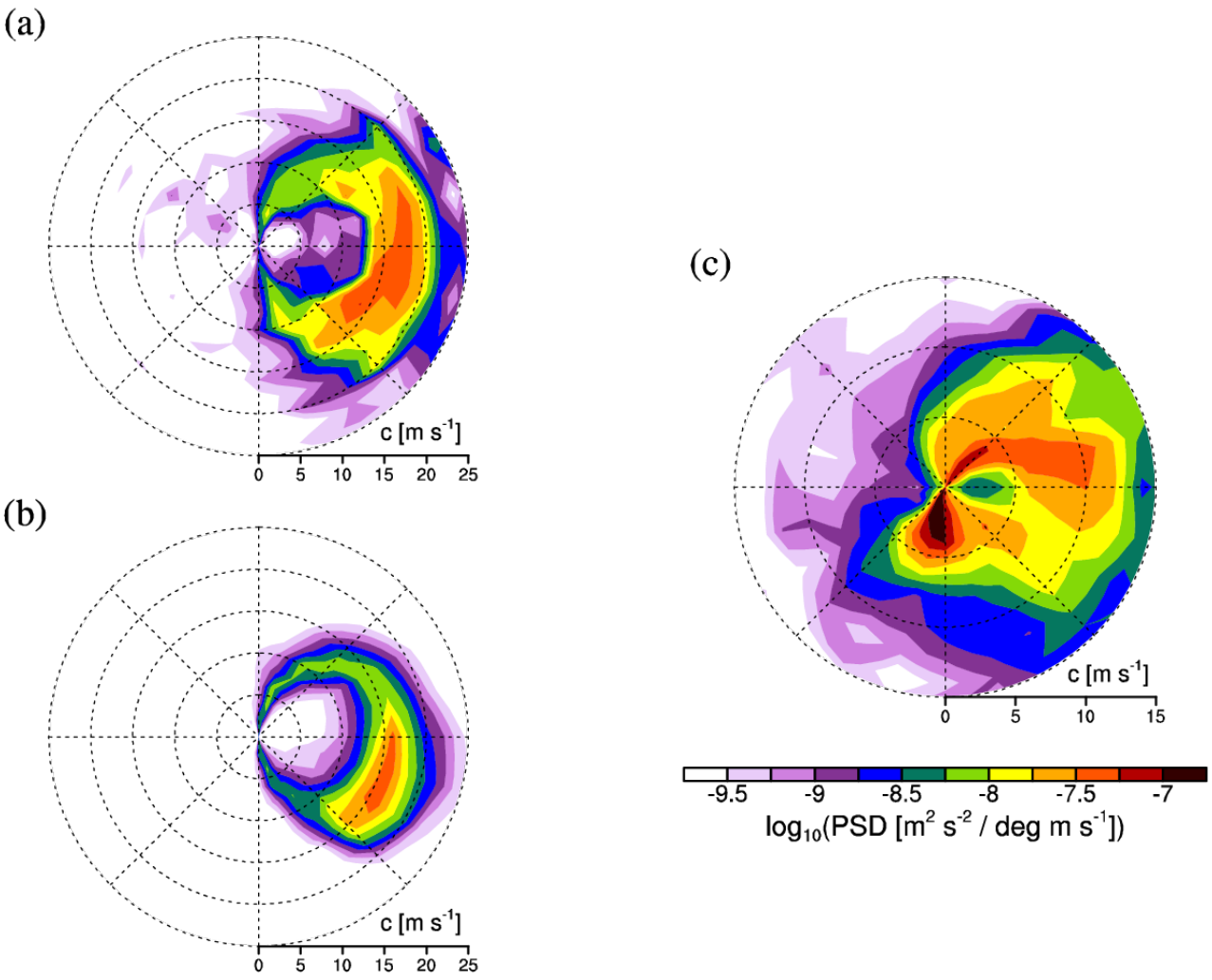
(a)
c [m s-1]
0 5 10 15 20 25
(b)
c [m s-1]
0 5 10 15 20 25
(c)
c [m s-1]
0 5 10 15
-9.5 -9 -8.5 -8 -7.5 -7
log10(PSD [m2 s-2 / deg m s-1])